Contract No. and Disclaimer:

This manuscript has been authored by Savannah River Nuclear Solutions, LLC under Contract No. DE-AC09-08SR22470 with the U.S. Department of Energy. The United States Government retains and the publisher, by accepting this article for publication, acknowledges that the United States Government retains a non-exclusive, paid-up, irrevocable, worldwide license to publish or reproduce the published form of this work, or allow others to do so, for United States Government purposes.

*Manuscript
Click here to view linked References

Single Phase Melt Processed Powellite $(Ba,Ca)MoO_4$ for the Immobilization of Mo-Rich Nuclear Waste

Kyle Brinkman [a, *], Kevin Fox [a], James Marra [a], Jason Reppert [a],

Jarrod Crum [b], Ming Tang [c]

[a] Savannah River National Laboratory, Aiken, SC 29808, USA

[b] Pacific Northwest National Laboratory, Richland, WA 99352 USA

[c] Los Alamos National Laboratory, Los Alamos, NM 87545 USA

Abstract

Crystalline and glass composite materials are currently being investigated for the immobilization of combined High Level Waste (HLW) streams resulting from potential commercial fuel reprocessing scenarios. Several of these potential waste streams contain elevated levels of transition metal elements such as molybdenum (Mo). Molybdenum has limited solubility in typical silicate glasses used for nuclear waste immobilization. Under certain chemical and controlled cooling conditions, a powellite $(Ba,Ca)MoO_4$ crystalline structure can be formed by reaction with alkaline earth elements. In this study, single phase $BaMoO_4$ and $CaMoO_4$ were formed from carbonate and oxide precursors demonstrating the viability of Mo incorporation into glass, crystalline or glass composite materials by a melt and crystallization process. X-ray diffraction, photoluminescence, and Raman spectroscopy indicated a long range ordered crystalline structure. In-situ electron irradiation studies indicated that both $CaMoO_4$ and $BaMoO_4$ powellite phases exhibit radiation stability up to 1000 years at anticipated doses with a crystalline to

amorphous transition observed after 1 X 10^{13} Gy. Aqueous durability determined from product consistency tests (PCT) showed low normalized release rates for Ba, Ca, and Mo (<0.05 g/m^2).

Keywords: waste form; nuclear materials; radiation damage; chemical durability

[*] Corresponding Author: (Tel.) 803-725-9843; (E-mail): kyle.brinkman@srnl.doe.gov

1. Introduction

Efforts being conducted by the United States Department of Energy (DOE) under the Fuel Cycle Research and Development (FCR&D) program are aimed at making the U.S. Fuel Cycle more effective by the development of next generation waste management technologies. Some fuel cycles being developed include the reprocessing of commercial used fuel in the U.S. The envisioned fuel reprocessing technology would separate the fuel into several fractions, thus, partitioning the waste into groups with common chemistry [1]. Immobilization of the High Level Waste (HLW) fraction may be achieved by chemical incorporation into the structure of a suitable matrix, typically a glass, glass – ceramic composite, or crystalline ceramic such that it is captured and unable to escape [2]. High level waste has been incorporated into borosilicate glass waste forms at the industrial scale for several decades and is an established technology [3-6].

Ceramic (or crystalline) phases incorporate the waste radionuclides as part of their crystal structure. Tailoring of ceramic phases is based on the knowledge that there are many naturally produced minerals containing radioactive and non-radioactive species very similar to the radionuclides of concern in wastes from fuel reprocessing [7]. This has led to the development of synthetic rock or SYNROC as coined by Ringwood et al. in 1979 [8, 9]. In addition, recent work has been increasingly focused on glass composite materials (GCM), intermediate between completely amorphous and fully crystalline materials. In these systems, the crystalline content and elemental partitioning may be controlled by glass forming additives and cooling rate [10-12]. Current work is aimed at developing a high throughput, reliable process for waste form processing. GCM waste

forms may be tailored to the projected combined fission product waste stream from commercial nuclear fuel reprocessing where actinides are removed via separations processes have the potential to meet the requisite waste loadings, ease of processing, radiation stability, chemical flexibility, and resistance to aqueous dissolution that are required for long term geologic storage.

Typically, crystalline materials for HLW immobilization have been densified via hot isostatic pressing [8]. However, recent work has shown that they can also be produced from a melt process analogous to GCM processing. For example, demonstrations have been completed using the Cold Crucible Induction Melter (CCIM) technology to produce several crystalline ceramic waste forms, including murataite-rich ceramics,[13, 14] zirconolite/pyrochlore ceramics,[15] Synroc-C (zirconolite, hollandite, perovskite),[16, 17] aluminotitanate ceramics, and zirconia [18]. This production route is advantageous since melters are already in use for commercial and defense high level waste (HLW) vitrification in several countries, and melter technology greatly reduces the potential for airborne contamination as compared to processes involving extensive powder handling operations. Production of GCM waste forms would be expected to be straightforward using the CCIM technology and demonstrations to this effect are currently underway.

The structure/property relations of individual phases within the multi-phase assemblage of GCM or ceramic waste forms are particularly important for the incorporation of challenging elements, such as molybdenum, which have low solubility in typical HLW glasses. These elements have concentrations in excess of 13 wt % in the projected

reprocessing waste streams. GCM waste forms are advantageous for the immobilization of these species since they form a stable phase within a glassy matrix [11]. A primary Mo containing crystalline phase that forms during GCM processing has been found to be a (Ba,Ca)MoO_4 powellite phase [5, 11]. These phases have been observed and studied as a component of a multiphase waste form system. However, little work has been performed on the melt processing and structure/property relations of single phase powellite materials from oxide and carbonate precursors. A systematic examination of single phase powellite materials including structure, radiation stability and aqueous durability provides a strong basis for understating current and future multiphase waste form systems.

Powellite is a molybdate mineral with a chemical formula of $CaMoO_4$ or $BaMoO_4$, and a tetragonal structure. Due to its structural variability, powellite can accommodate considerable chemical substitutions including trivalent actinides and lanthanide elements [19]. Lanthanide-doped $CaMoO_4$ single crystals have been studied for their luminescent optical properties [20]. Barium molybdate ($BaMoO_4$) is a promising catalyst for oxidation of soot particulates,[21] and an additive for corrosion inhibiting pigments [22]. Due to Mo-O and Mo-Mo bonds in the structure, it is also of interest for electronic properties such as phosphor-converted light emitting diodes (LEDs) [23, 24]. It is noted that luminescence spectroscopy of waste forms may also reveal elemental partitioning in distinct phases by measuring UV stimulated visible emissions from rare earth elements (Nd, Sm, Gd) as well as molybdate structures (MoO_4^{2-}). The latter has been performed to investigate what happens after dissolution of a primary waste form containing Eu and

Cm. Results indicated the feasibility of re-incorporation into natural occurring minerals such as aragonite, a metastable $CaCO_3$ frequently found in nature [25]. Raman spectroscopy has been used in borosilicate glasses containing MoO_3 to track the alkali and alkaline earth molybdate crystallization during melt cooling and examine the variation of MoO_4^{2-} environment in the glass structure [26]. This present work uses Raman spectroscopy to investigate the structure of melt processed single phase $BaMoO_4$, $CaMoO_4$, and demonstrates the potential utility to map molybdate content in combined waste forms [27].

Powellite $CaMoO_4$ has been investigated in aqueous environments in order to better understand the fate and behavior of molybdenum in spent oil shale disposal environments [28]. It was found that $CaMoO_4$ does not control molybedenum concentrations in spent oil suggesting the potential for good aqueous durability with respect to Mo leaching; however there has not been extensive testing with standard corrosion tests used in waste form characterization. The radiation effects in multiphase ceramic and GCM waste forms have been initiated, however little is known regarding the behavior of crystalline molybdate materials such as powellite [29, 30].

This work aims to i) investigate $BaMoO_4$ and $CaMoO_4$ powellite single phase formation and morphology produced from a melt and crystallize process which simulates expected processing conditions of fully crystalline and composite glass/ceramic waste forms, ii) examine the durability of Mo containing powellite phase to aqueous environments, and iii) evaluate the radiation stability of powellite crystalline phases.

2. Experimental

The materials synthesis focus was to prepare single phase $CaMoO_4$ and $BaMoO_4$ from a melt process using oxide and carbonate precursors for subsequent structure/property investigations. Powders of 99.5% pure calcium carbonate ($CaCO_3$), barium carbonate ($BaCO_3$) and molybdenum oxide (MoO_3) from Aldrich (Milwaukee, WI) were used as precursors for powellite material synthesis. The powders were weighed in stoichiometric ratios and were ball milled in ethyl alcohol in an alumina jar with alumina milling media for four hours followed by drying overnight at 70°C. Samples of each of the batch materials were melted in an electric resistance heated furnace to simulate melter production. The blended and dried powders were placed into Pt/Rh alloy crucibles and melted at 1500°C for 20 minutes. Power to the furnace was then turned off with the crucibles remaining inside to cool slowly (furnace cooling) to roughly approximate the slow cooling conditions experienced by a waste form poured from a melter into a canister. The phase development of the samples prepared from melts was compared with the crystalline phases formed from powder batches calcined at 900 to 1100 °C for four hours. Representative samples were ground and analyzed by XRD from 10 to 80 degrees two theta using CuKα (1.5418 Å) on a PANalytical X-ray diffractometer (Almelo, The Netherlands).

Representative samples of select compositions were characterized to confirm that the as-fabricated powellite ceramics met the targeted compositions and to assess the potential volatility issues. The samples were prepared using lithium-metaborate fusions followed

by acid dissolution. The resulting solutions were analyzed by Inductively Coupled Plasma – Atomic Emission Spectroscopy (ICP-AES). Two measurements were taken for each element of interest, and the average of these two measurements was taken as the measured value.

Most of the self-irradiation in a waste form incorporating fission products is due to beta particle and gamma emission. These emissions cause radiation damage primarily via radiolytic processes, because both beta and gamma particles induce substantial electronic excitations in a target material. Electrons provide a useful means to examine radiolysis effects because electrons deposit nearly all of their energy in solids via electronic loss processes. In this study, the researchers used electron irradiations to simulate the self-radiation damage that occurs in a material incorporating nuclides undergoing radioactive decay. *In situ* electron irradiations were performed using 300-keV electrons generated in a FEI Tecnai F30 transmission electron microscope (TEM) (FEI Company, Hillsboro, OR). Powellite samples were crushed and suspended on a holey-carbon film supported by copper grids. Electron irradiation experiments were carried out by focusing the electron beam onto small regions of electron transparent material (a typical irradiated region was ~100 nm diameter). During these electron beam irradiation experiments, the incident electron flux, measured using a faraday cup, was approximately 1.6×10^{24} e/m^2 s. Irradiations were performed up to a fluence of 1×10^{27} e/m^2(corresponding to a dose of 1.5×10^{13} Gy).

Raman spectra were recorded using a Renishaw InVia Raman spectrometer (Gloucestershire, United Kingdom) equipped with a 532 nm laser light source and using a spectral resolution of 3 cm^{-1}. Each sample was scanned for 20 seconds using a laser power of ~5 mW. For photoluminescence measurements (JY FluoroMax-4, HORIBA Jobin Yvon Inc., Edison, NJ), a xenon light source was used to excite the samples in the UV region (260 – 390 nm). Each spectrum was recorded with a 0.5 second integration time in 1 nm intervals.

The ASTM C1285 Product Consistency Test (PCT) Method B was used to provide a preliminary measure of the chemical durability of the ceramic waste forms.[31] Samples of each waste form were ground to less than 100 mesh using a tungsten carbide grinder. All of the fine particulates were used in the PCT due to the small quantities of material available. The surface areas of each individual sample were determined using Brunauer-Emmett-Teller (BET) analysis (Micromeritics ASAP 2020, Norcross, GA) with nitrogen or krypton as the analysis gas prior to performing the PCT. No washing steps were performed since the removal of fine particles would invalidate the BET results. The PCT Method-B was performed on the selected samples in two sets. Also included were samples of the Approved Reference Material (ARM) glass, the Environmental Assessment (EA) glass, and blanks from the vessel cleaning batches. Stainless steel vessels were used with 15 ml of Type-I ASTM water and 1.5 g of the ground sample. The vessels were sealed placed in an oven at 90 °C for 7 days. Once cooled, the resulting solutions were filtered and acidified, then analyzed by ICP-AES. Normalized release rates were calculated based on the measured compositions using the averages of the

common logarithms of the leachate concentrations measured against the amount of exposed sample surface area using the BET surface area measurements.

3. Results and Discussion

Figure 1 displays the calculated free energy (kJ/mol) change for $BaMoO_4$ and $CaMoO_4$ powellite formation from carbonate and oxide precursors versus temperature [32]. The calcium containing powellite structure $CaMoO_4$ has a more negative enthalpy of formation (-1542 kJ/mol versus -1507 for $BaMoO_4$) and a more negative free energy of formation, resulting in the preferred powellite structure. Multi-phase glass ceramic compositions with high levels of Mo frequently demonstrate crystalline $CaMoO_4$ formation upon cooling [11]. However, $BaMoO_4$ has also been observed in both ceramic and glass ceramic waste forms [33]. In addition, there is a solid solution present in the $Ba_{1-x}Ca_xMoO_4$ system, which makes the study of the single phase $CaMoO_4$ and $BaMoO_4$ powellite end members a worthwhile pursuit [34].

Figure 2 displays the XRD pattern of $BaMoO_4$ and $CaMoO_4$ fabricated from carbonate and oxide precursors by melting at 1500 °C for 20 minutes followed by furnace cooling. Single phase powellite with the scheelite structure was observed with lattice parameters a=b=5.23 Å, c=11.43 Å for $CaMoO_4$ and a=b=5.58 Å, c=12.82 Å for $BaMoO_4$. Figure 3 and 4 displays the TEM bright field (BF) image, selected area electron diffraction (SAED) and Energy-dispersive X-ray spectroscopy (EDS) spectrum of $CaMoO_4$ and $BaMoO_4$ respectively indicating the single phase nature and appropriate stoichiometry. The lattice parameter of $CaMoO_4$ based on d-spacing data from SAED were calculated as

a=b=5.27 Å, c=11.49 Å and the $BaMoO_4$ SAED determined lattice parameters were calculated as a=b=5.61 Å, c=12.83 Å. Both values TEM SAED values agree well with structural parameters determined from XRD.

The single phase powellite materials fabricated in this study had larger a=b and c lattice parameters than literature values for powellite materials formed during multiphase waste form processing in the presence of lanthanide elements [33]. This is believed to be due to the partial substitution of Ca^{+2} and Ba^{+2} for smaller lanthanide series elements such as Tb^{+3}, Gd^{+3} and concomitant point defect compensation including the formation of negatively charged barium vacancy (V_{Ba}'') required to compensate the ($M^{+3}_{Ba+2}\bullet$) donor substitution [35].

Figure 5 displays the results of a series of *in situ* electron irradiations on single phase $CaMoO_4$ and Figure 6 displays the analogous results for $BaMoO_4$. The high resolution electron microscopy (HREM) images along with its fast Fourier transformation (FFT) diffractograms clearly show the microstructural evolution of an irradiated area. The high resolution images indicate that a crystalline to amorphous transition occurred after 10^{13} Gy. These results suggest that the powellite phase materials exhibit stability to 1000 years at anticipated doses (2×10^{10}-2×10^{11} Gy) based on current commercial HLW glasses [1]. The structural change was observed on *in situ* electron irradiated $CaMoO_4$ and $BaMoO_4$ after 10^{13} Gy which suggests both powellite materials have similar radiation stability upon β-particles and γ-emissions. It is noted that actual self-irradiation during waste form storage would come from β-particles fluxes which are orders of magnitude

lower than that used in TEM irradiation experiments. Whether similar radiation damage and defect generation processes occur with low flux, long duration β-particles exposure as compared to high flux, short duration exposure to electrons in TEM experiments requires careful studies and is the subject of substantial current efforts.

The photoluminescence (PL) of molybdates such as $BaMoO_4$ have been reported in thin film and powder form as a function of structural disorder [36-38]. It has been observed that materials which are structurally disordered possess defects such as oxygen vacancies, lattice defects, impurities, and local bond distortions which yield localized electronic levels in the band gap [39]. These electronic levels are responsible for enhancing PL emission in disordered materials. Figure 7 displays the PL spectra for $CaMoO_4$ single phase powders calcined at 1100 °C for 4 hours. The excitation spectrum in Figure 7a shows distinct absorptions at the 375, 405 and 430 nm, wavelengths characteristic of $[MoO_4]^{2-}$ tetrahedral absorptions. The emission spectrum of the powders in Figure 7b shows emissions between 425 and 470 nm confirming the presence of a crystalline, ordered phase and concomitant energy levels associated with visible light emission. Addition of rare earth elements present in the waste stream could lead to partial substitution on the Ca^{+2} or Ba^{+2} site promoting disorder in the system and favoring PL emission [30]. Therefore, photoluminescent measurements may be a relatively easy way to evaluate powellite formation and purity in a multiphase GCM waste form.

Raman spectroscopy is an effective tool for examining the degree of structural disorder. Disordered crystals exhibit deviations including broadening and shifting of the peaks, the

appearance of peak splitting, and peaks normally forbidden by bulk crystal symmetry. For the (Ba,Ca)MoO_4 system, vibrations within the $[MoO_4]^{2-}$ tetrahedral clusters give rise to internal vibrational modes. External modes or lattice phonons arise from $[BaO_8]$ clusters and from rigid molecular unit $[MoO_4]^{2-}$ clusters. The Raman peaks appearing in Figure 8 at 325, 792, 838 and 880 cm^{-1} are indicative of internal MoO_4 vibrations in crystalline (Ba,Ca)MoO_4. The Raman peaks at 393 and 407 cm^{-1} in $CaMoO_4$ and 347 and 360 cm^{-1} for $BaMoO_4$ are associated with internal MoO_4 vibrations in the structure [40]. Deviations from the peak center (> 3 cm^{-1}, the resolution of the instrument) could be the result of different bond lengths and interactions between Ca , Ba and MoO_4 [41, 42]. The peaks below 200 cm^{-1} are indicative of external vibrations indicating a high degree of crystallinity and long range order. Table 1 lists the vibrational modes and Raman peaks as observed in this study These results demonstrates the utility of vibrational spectroscopy in monitoring molybdenum incorporation and powellite phase formation nuclear waste forms.

The results of the chemical composition measurements for the crystalline powellite phases are given along with their targeted values in Table 2. The measured concentrations are reasonably close to their targeted values for the $CaMoO_4$ and $BaMoO_4$ compositions. Of particular interest is that both powellite phases retained approximately 95% of the targeted Mo concentrations after the melt and crystallization process indicating relatively low volatility of Mo from the melt. These composition measurements were used in normalizing the PCT data. The sum of the measured oxide composition is less than 100% due to incomplete dissolution in the acid solutions

employed in PCT durability measurements. The constant ratio of Ca/Mo and Ba/Mo in the targeted and measured values indicates incomplete dissolution.

The PCT results for the single phase $BaMoO_4$ and $CaMoO_4$ samples are shown in Table 3. The powellite phases had very low normalized release values for Ba, Ca, (<0.01 g/m^2) and Mo (< 0.05 g/m^2). Figure 9 shows the calculated free energy of dissolution reaction of the powellite to M^{2+} and MoO_4^{2-} ions in aqueous solution versus temperature [32]. The positive value for the free energy change and increasing value with increasing temperature indicate that the dissolution reaction is unfavorable. Figure 9 also displays the free energy of formation of Na^+ and Cl^+ from NaCl showing known favorable thermodynamics for dissolution. This behavior is similar to alkali molybdates such as Na_2MoO_4 which are known to be water soluble. Multi-phase waste form composition and processing should be tailored to avoid these secondary phases [26]. Collectively these experiments indicate that the chemical durability of the individual $BaMoO_4$ and $CaMoO_4$ phases is promising and melt processing of waste forms containing Mo and Ba fission products into crystalline $BaMoO_4$ and $CaMoO_4$ phases in glass ceramic composite is a feasible method for high level waste treatment. Further work will involve the systematic incorporation of lanthanide and selected actinide elements into powellite materials and a comparison between materials formed in single phase experiments versus compounds formed in multi-phase waste forms that may incorporate a variety of dopants.

4. Conclusion

Single phase $BaMoO_4$ and $CaMoO_4$ were formed by melt processing carbonate and oxide precursors. X-ray diffraction indicated that desired powellite phase was formed via the melt and crystallize route. PL and Raman spectroscopy indicated highly crystalline materials with modes associated with long range order. PL and Raman measurements of $(Ba,Ca)MoO_4$ were sensitive to MoO_4^{2-} tetrahedra environments indicating that these measurements may be an effective and easy means to measure in-situ powellite formation during melt processing of a multiphase GCM waste form. In-situ electron irradiation studies indicated that the powellite phase exhibits radiation stability up to 1000 years at anticipated doses with a crystalline to amorphous transition observed after 10^{13} Gy. Chemical composition measurements showed very low volatile losses of Mo after melting at 1500 °C, supporting the viability of a melt and crystallize production method for single phase powellite from oxide and carbonate precursors. Aqueous durability determined from product consistency tests (PCT) showed low normalized release rates for Ba, Ca, Mo (<0.05 g/m^2) indicating appreciable chemical durability.

Acknowledgements

This document was prepared in conjunction with work accomplished under Contract No. DE-AC09-08SR22470 with the U.S. Department of Energy. The authors acknowledge gratefully the financial support of the DOE-NE Separations and Waste Form program. A. Mendez-Torres and D. Missimer gratefully acknowledged for processing and characterization work.

References

[1] W.J. Weber, A. Navrotsky, S. Stefanovsky, E.R. Vance, E. Vernaz, Materials Science of High-Level Nuclear Waste Immobilization, MRS Bull., 34 (2009) 46-53.
[2] Waste Forms Technology and Performance Final Report by National Research Council of the National Academies ISBN-10: 0-309-18733-8, Waste Forms Technology and Performance Final Report by National Research Council of the National Academies ISBN-10: 0-309-18733-8, (2011).
[3] M.I. Ojovan, W.E. Lee, An introduction to nuclear waste immobilisation, Oxford, Elsevier, (2005).
[4] J.D. Vienna, Nuclear Waste Vitrification in the United States: Recent Developments and Future Options, International Journal of Applied Glass Science, 1 (2010) 309-321.
[5] P.B. Rose, D.I. Woodward, M.I. Ojovan, N.C. Hyatt, W.E. Lee, Crystallisation of a simulated borosilicate high-level waste glass produced on a full-scale vitrification line, J. Non-Cryst. Solids, 357 (2011) 2989-3001.
[6] C.L. Crawford, J.C. Marra, N.E. Bibler, Glass fabrication and product consistency testing of lanthanide borosilicate glass for plutonium disposition, J. Alloy. Compd., 444 (2007) 569-579.
[7] W.E. Lee, M.I. Ojovan, M.C. Stennett, N.C. Hyatt, Immobilisation of radioactive waste in glasses, glass composite materials and ceramics, Adv. Appl. Ceram., 105 (2006) 3-12.
[8] A.E. Ringwood, S.E. Kesson, N.G. Ware, W. Hibberson, A. Major, IMMOBILIZATION OF HIGH-LEVEL NUCLEAR-REACTOR WASTES IN SYNROC, Nature, 278 (1979) 219-223.
[9] A.E. Ringwood, S.E. Kesson, N.G. Ware, W.O. Hibberson, A. Major, SYNROC PROCESS - GEOCHEMICAL APPROACH TO NUCLEAR WASTE IMMOBILIZATION, Geochem. J., 13 (1979) 141-165.
[10] P. Loiseau, D. Caurant, N. Baffier, L. Mazerolles, C. Fillet, Glass-ceramic nuclear waste forms obtained from SiO(2)-Al(2)O(3)-CaO-ZrO(2)-TiO(2) glasses containing lanthanides (Ce, Nd, Eu, Gd, Yb) and actinides (Th): study of internal crystallization, J. Nucl. Mater., 335 (2004) 14-32.
[11] N. Henry, P. Deniard, S. Jobic, R. Brec, C. Fillet, F. Bart, A. Grandjean, O. Pinet, Heat treatments versus microstructure in a molybdenum-rich borosilicate, J. Non-Cryst. Solids, 333 (2004) 199-205.
[12] T. Taurines, B. Boizot, Synthesis of powellite-rich glasses for high level waste immobilization, J. Non-Cryst. Solids, 357 (2011) 2723-2725.
[13] S.V. Stefanovsky, A.G. Ptashkin, O.A. Knyazev, S.A. Dmitriev, S.V. Yudintsev, B.S. Nikonov, Inductive Cold Crucible Melting of Actinide-bearing Murataite-based Ceramics, Journal of Alloys and Compounds, 444-445 (2007) 438-442.
[14] J. Lian, L.M. Wang, R.C. Ewing, S.V. Yudintsev, S.V. Stefanovsky, Thermally induced phase decomposition and nanocrystal formation in murataite ceramics, J. Mater. Chem., 15 (2005) 709-714.
[15] A.V. Demine, N.V. Krylova, P.P. Polyektov, I.N. Shestoperov, T.V. Smelova, V.F. Gorn, G.M. Medvedev, High Level Waste Solidification Using a Cold Crucible Induction Melter, in: K.P. Hart, G.R. Lumpkin (Eds.), 2001, pp. 27-34.

[16] I.A. Sobolev, S.V. Stefanovskii, F.A. Lifanov, SYNTHESIS OF A SYNROC CERAMIC FROM THE MELT, Radiochemistry, 35 (1993) 330-336.
[17] H.F. Xu, X.F. Wang, Crystallization sequence and microstructure evolution of Synroc samples crystallized from CaZrTi2O7 melts, J. Nucl. Mater., 279 (2000) 100-106.
[18] G. Leturcq, T. Advocat, K. Hart, G. Berger, J. Lacombe, A. Bonnetier, Solubility Study of Ti Zr-based Ceramics Designed to Immobilize Long-lived Radionuclides, American Mineralogist, 86 (2001) 871-880.
[19] D. Bosbach, T. Rabung, F. Brandt, T. Fanghanel, Trivalent actinide coprecipitation with powellite (CaMoO4): Secondary solid solution formation during HLW borosilicate-glass dissolution, Radiochim. Acta, 92 (2004) 639-643.
[20] L.H.C. Andrade, M.S. Li, Y. Guyot, A. Brenier, G. Boulon, Optical multi-sites of Nd3+-doped CaMoO4 induced by Nb5+ charge compensator, J. Phys.-Condes. Matter, 18 (2006) 7883-7892.
[21] M.A. Hasan, M.I. Zaki, K. Kumari, L. Pasupulety, Soot deep oxidation catalyzed by molybdena and molybdates: a thermogravimetric investigation, Thermochim. Acta, 320 (1998) 23-32.
[22] D.R. Robitaille, M.S. Vukasovich, H.F. Barry, US Patent No. 3 969 127; Appl. No. 1975-556593, US Patent No. 3 969 127; Appl. No. 1975-556593 (1976).
[23] A.P. Kiselev, S.Z. Shmurak, B.S. Red'kin, V.V. Sinitsyn, I.M. Shmyt'ko, E.A. Kudrenko, E.G. Ponyatovskii, Evolution of the spectral response of amorphous europium molybdate under annealing, Phys. Solid State, 48 (2006) 1544-1552.
[24] R. Lam, G. Blasse, LUMINESCENCE OF BARIUM MOLYBDATE (BAMOO4), J. Chem. Phys., 71 (1979) 3549-3549.
[25] M. Schmidt, T. Stumpf, C. Walther, H. Geckeis, T. Fanghanel, Incorporation versus adsorption: substitution of Ca(2+) by Eu(3+) and Cm(3+) in aragonite and gypsum, Dalton Trans., (2009) 6645-6650.
[26] D. Caurant, O. Majerus, E. Fadel, A. Quintas, C. Gervais, T. Charpentier, D. Neuville, Structural investigations of borosilicate glasses containing MoO3 by MAS NMR and Raman spectroscopies, J. Nucl. Mater., 396 (2010) 94-101.
[27] V. Panchal, N. Garg, S.M. Sharma, Raman and x-ray diffraction investigations on BaMoO4 under high pressures, J. Phys.-Condes. Matter, 18 (2006) 3917-3929.
[28] M.E. Essington, CALCIUM MOLYBDATE SOLUBILITY IN SPENT OIL-SHALE AND A PRELIMINARY EVALUATION OF THE ASSOCIATION CONSTANTS FOR THE FORMATION OF CAMOO40(AQ), KMOO4-(AQ), AND NAMOO4-(AQ), Environ. Sci. Technol., 24 (1990) 214-220.
[29] W.J. Weber, R.C. Ewing, C.R.A. Catlow, T.D. de la Rubia, L.W. Hobbs, C. Kinoshita, H. Matzke, A.T. Motta, M. Nastasi, E.K.H. Salje, E.R. Vance, S.J. Zinkle, Radiation effects in crystalline ceramics for the immobilization of high-level nuclear waste and plutonium, J. Mater. Res., 13 (1998) 1434-1484.
[30] C. Mendoza, D. de Ligny, G. Panczer, S. Peuget, I. Bardez-Giboire, S. Schuller, Behaviour of the Eu3+ D-5(0) -> F-7(0) transition in CaMoO4 powellite type ceramics under Ar and Pb ions implantation, Opt. Mater., 34 (2011) 386-390.
[31] ASTM C1285-02(2008) Standard Test Methods for Determining Chemical Durability of Nuclear, Hazardous, and Mixed Waste Glasses and Multiphase Glass Ceramics: The Product Consistency Test (PCT).

[32] HSC, in, HSC, A Chemical Reaction and Composition Equilibrium Code, Outokumpu Research, Oy, Pori, Finland.
[33] K. Brinkman, K. Fox, M. Tang, Development of Crystalline Ceramics for Immobilization of Advanced Fuel Cycle Reprocessing Wastes, Savannah River National Laboratory Technical Report: SRNL-STI-2011-00516, FCRD-SWF-2011-000310, (2011).
[34] P. Yu, J. Bi, D.J. Gao, D.Q. Xiao, L.P. Chen, X.L. Jin, Z.N. Yang, Study of polycrystalline Ba(1-x)Ca(x)MoO(4) films prepared by electrochemical technique, J. Electroceram., 21 (2008) 184-188.
[35] A.P.D. Marques, F.V. Motta, M.A. Cruz, J.A. Varela, E. Longo, I.L.V. Rosa, BaMoO4:Tb+3 phosphor properties: Synthesis, characterization and phtophysical studies, Solid State Ionics, 201 (2011) 54-59.
[36] X.Y. Wu, J. Du, H.B. Li, M.F. Zhang, B.J. Xi, H. Fan, Y.C. Zhu, Y.T. Qian, Aqueous mineralization process to synthesize uniform shuttle-like BaMoO4 microcrystals at room temperature, J. Solid State Chem., 180 (2007) 3288-3295.
[37] A.P.A. Marques, D.M.A. de Melo, E. Longo, C.A. Paskocimas, P.S. Pizani, E.R. Leite, Photoluminescence properties of BaMoO4 amorphous thin films, J. Solid State Chem., 178 (2005) 2346-2353.
[38] C.H. Cui, J. Bi, F. Shi, X. Lai, D.J. Gao, Unique photoluminescence properties of highly crystallized BaMoO4 film prepared by chemical reaction, Mater. Lett., 61 (2007) 4525-4527.
[39] A.P.A. Marques, F.C. Picon, D.M.A. Melo, P.S. Pizani, E.R. Leite, J.A. Varela, E. Longo, Effect of the order and disorder of BaMoO4 powders in photoluminescent properties, J. Fluoresc., 18 (2008) 51-59.
[40] E. Sarantopoulou, C. Raptis, S. Ves, D. Christofilos, G.A. Kourouklis, Temperature and pressure dependence of Raman-active phonons of CaMoO4: an anharmonicity study, J. Phys.-Condes. Matter, 14 (2002) 8925-8938.
[41] S.B. Xie, K.D. Chen, A.T. Bell, E. Iglesia, Structural characterization of molybdenum oxide supported on zirconia, J. Phys. Chem. B, 104 (2000) 10059-10068.
[42] A.P.D. Marques, D.M.A. de Melo, C.A. Paskocimas, P.S. Pizani, M.R. Joya, E.R. Leite, E. Longo, Photoluminescent BaMoO4 nanopowders prepared by complex polymerization method (CPM), J. Solid State Chem., 179 (2006) 671-678.

Figure captions

Figure 1. Free energy (G kJ/mol) changes with reaction from carbonate and oxide precursors for the formation of $CaMoO_4$ and $BaMoO_4$ versus temperature.

Figure 2. X-ray diffraction (XRD) patterns of single phase $CaMoO_4$ and $BaMoO_4$ formed by melting carbonate and oxide precursors at 1500^oC.

Figure 3 a) TEM bright field image and SAED and b) EDS of melt processed $CaMoO_4$

Figure 4 a) TEM bright field image and SAED and b) EDS of melt processed $BaMoO_4$

Figure 5 High resolution transmission electron microscopy image of $CaMoO_4$ a) before electron irradiation including FFT diffraction b) 5×10^{12} Gy, c) High resolution image and FFT indicating amorphous transition at 1.5×10^{13} Gy.

Figure 6 High resolution transmission electron microscopy image of $BaMoO_4$ a) before electron irradiation including FFT diffraction b) 5×10^{12} Gy, c) High resolution image and FFT indicating amorphous transition at 1.5×10^{13} Gy.

Figure 7. Photoluminescence of $CaMoO_4$ a) excitation spectrum and b) emission spectrum

Figure 8. Raman spectra of $CaMoO_4$, and $BaMoO_4$

Figure 9. Aqueous stability determined by free energy (kJ/mol) versus temperature for dissolution reaction

Table captions

Table 1. $(Ba,Ca)MoO_4$ vibrational modes and Raman peaks

Table 2. Targeted and Measured Compositions (wt %) of the Powellite Phases Fabricated by Melting and Crystallizing.

Table 3. Normalized release (g/m^2) as measured by product consistency test (PCT)

Note- both powellite phases retained 95% of the targeted Mo concentrations after melting and crystallizing

Table 1. (Ba,Ca)MoO_4 vibrational modes and Raman peaks

Vibrational Mode	**Raman Peaks (cm^{-1})**	
	$CaMoO_4$	$BaMoO_4$
$\nu_1 (2A_1)$	879	892
$\nu_3 (2F_2)$	848, 795	838, 792
$\nu_4 (2F_2)$	407, 393	360, 347
$\nu_2 (2E)$	324	325
$\nu_{f.r} (2F_1)$ free rotation	208	190
ν_{ext} –external modes MoO_4^{2-} and Ca^{+2}/Ba^{+2} motion	146, 114	142, 110

Table 2. Targeted and Measured Compositions (wt %) of the Powellite Phases Fabricated by Melting and Crystallizing.

Oxide	$CaMoO_4$		$BaMoO_4$	
	Targeted wt. %	**Measured wt. %**	**Targeted wt. %**	**Measured wt. %**
BaO	-	-	51.6	48.3
CaO	28.0	26.5	-	-
MoO_3	72.0	68.0	48.4	46.1
Sum	100.0	94.5	100.0	94.4

Table 3. Normalized release (g/m^2) as measured by product consistency test (PCT)

Note- both powellite phases retained 95% of the targeted Mo concentrations after melting and crystallizing

Composition	Ba	Ca	Mo
$CaMoO_4$	-	0.00	0.01
$BaMoO_4$	0.01	-	0.05

Figure1

Click here to download high resolution image

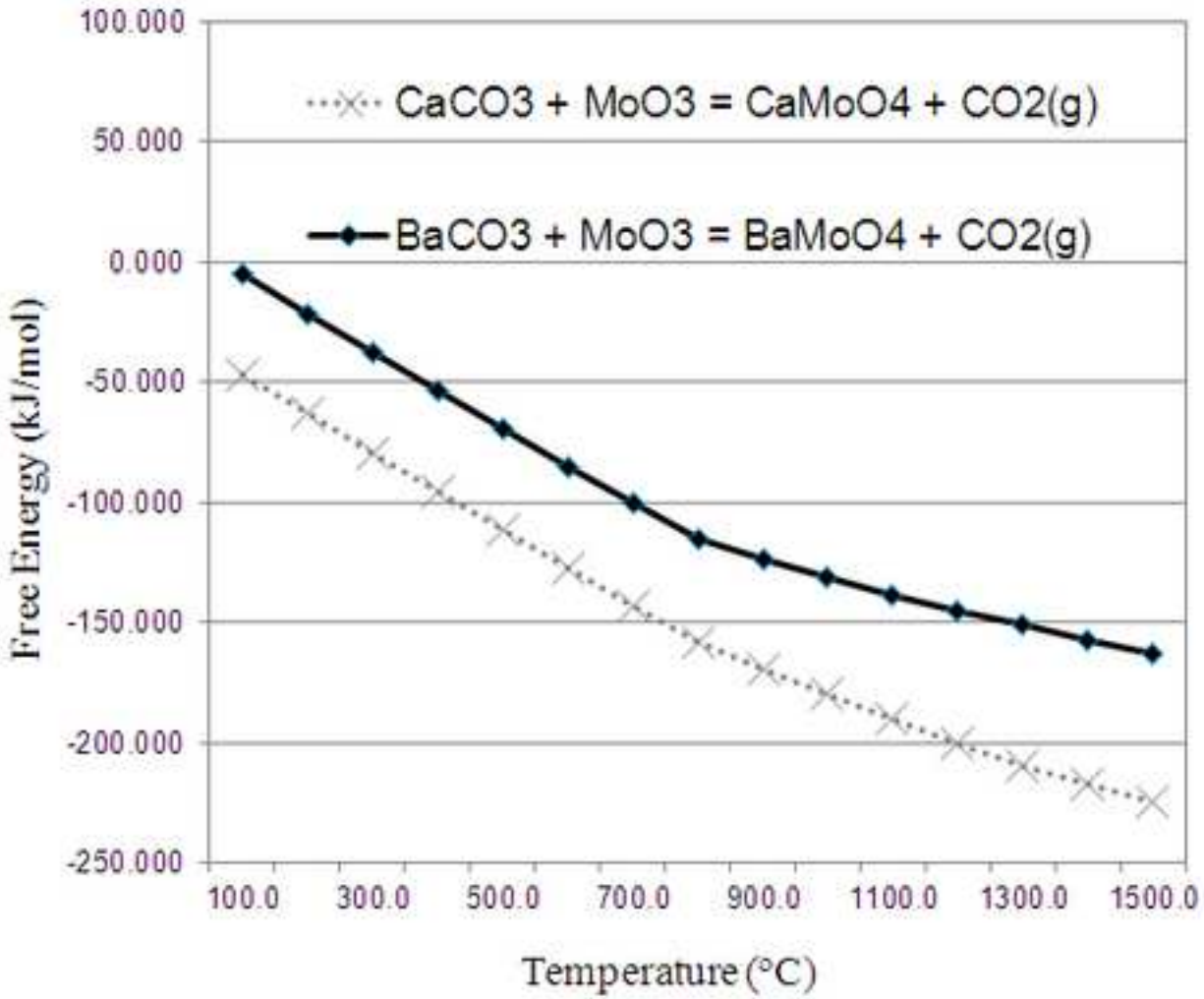

Figure2

Click here to download high resolution image

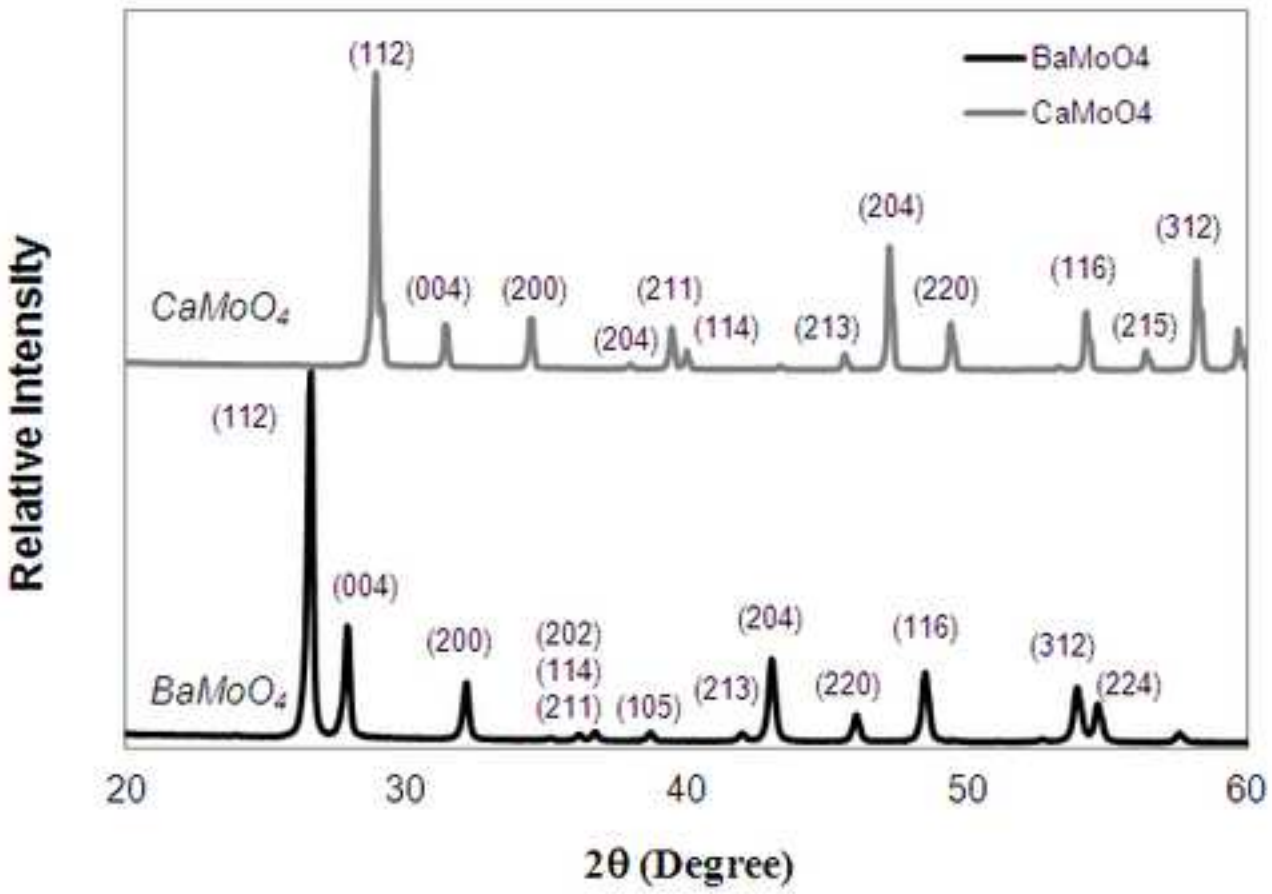

Figure3

Click here to download high resolution image

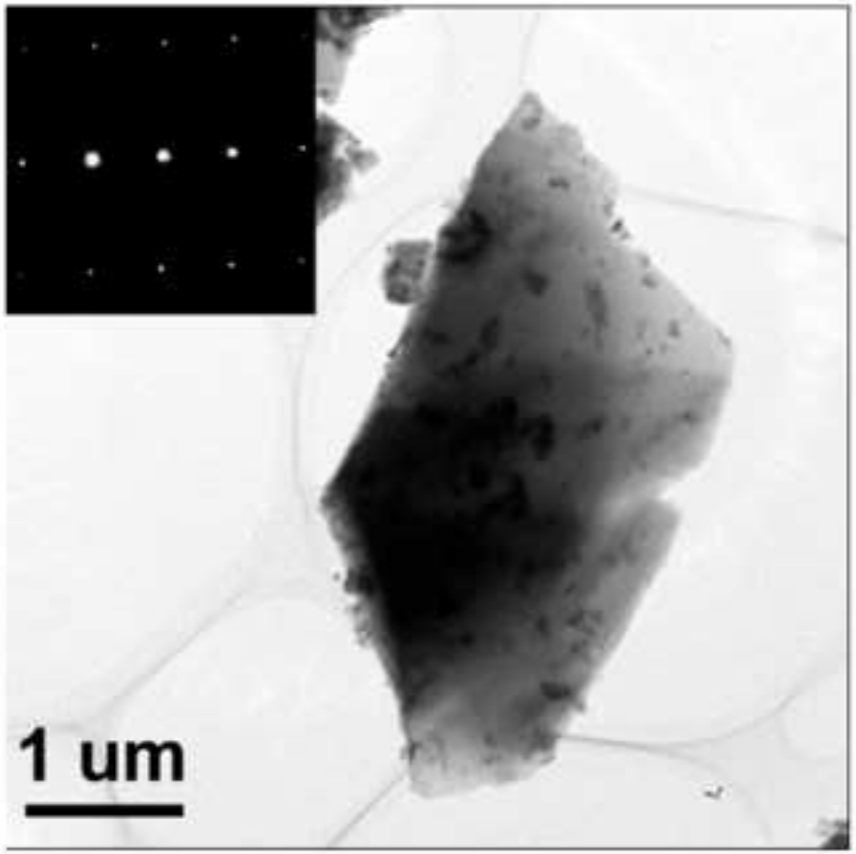

a)

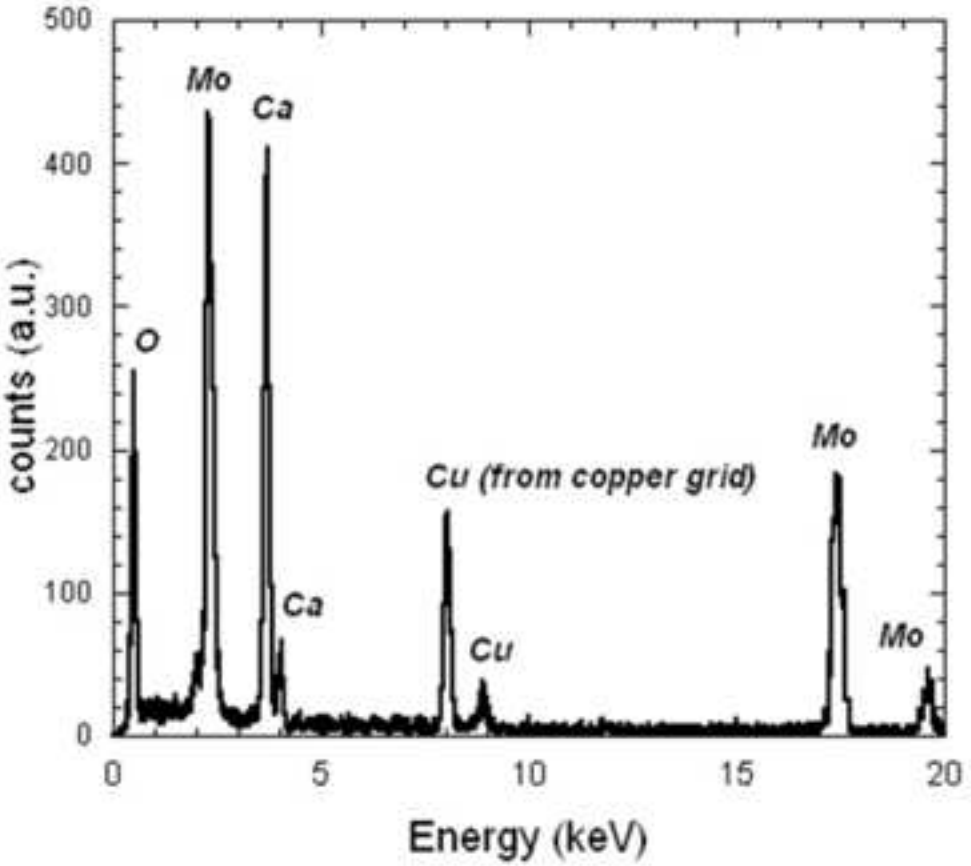

b)

Figure4

Click here to download high resolution image

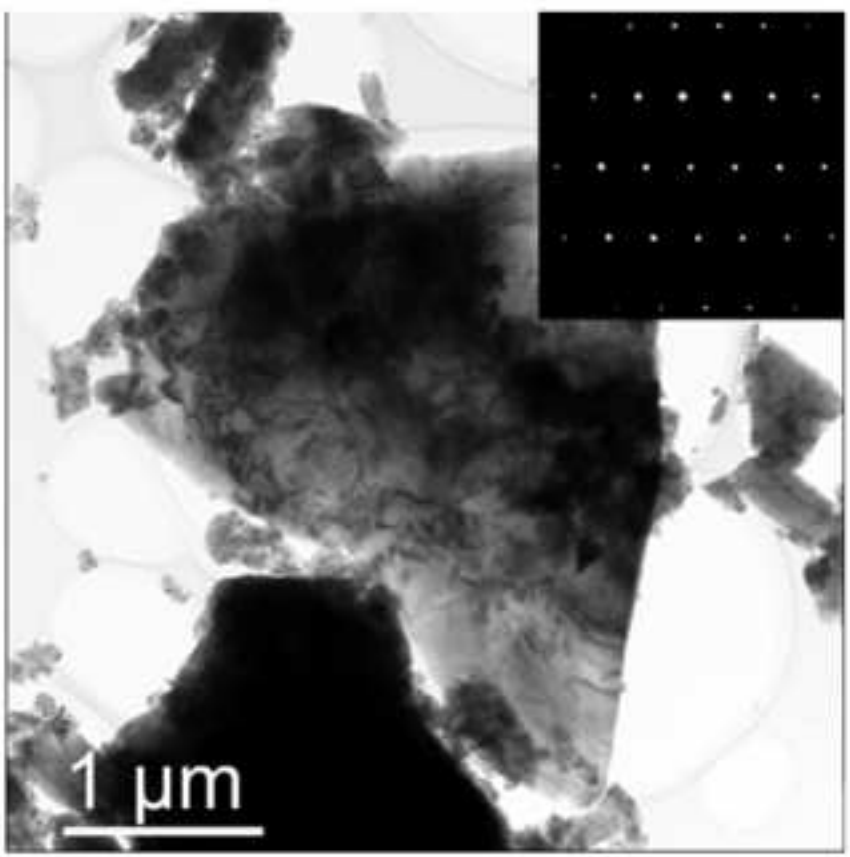

a)

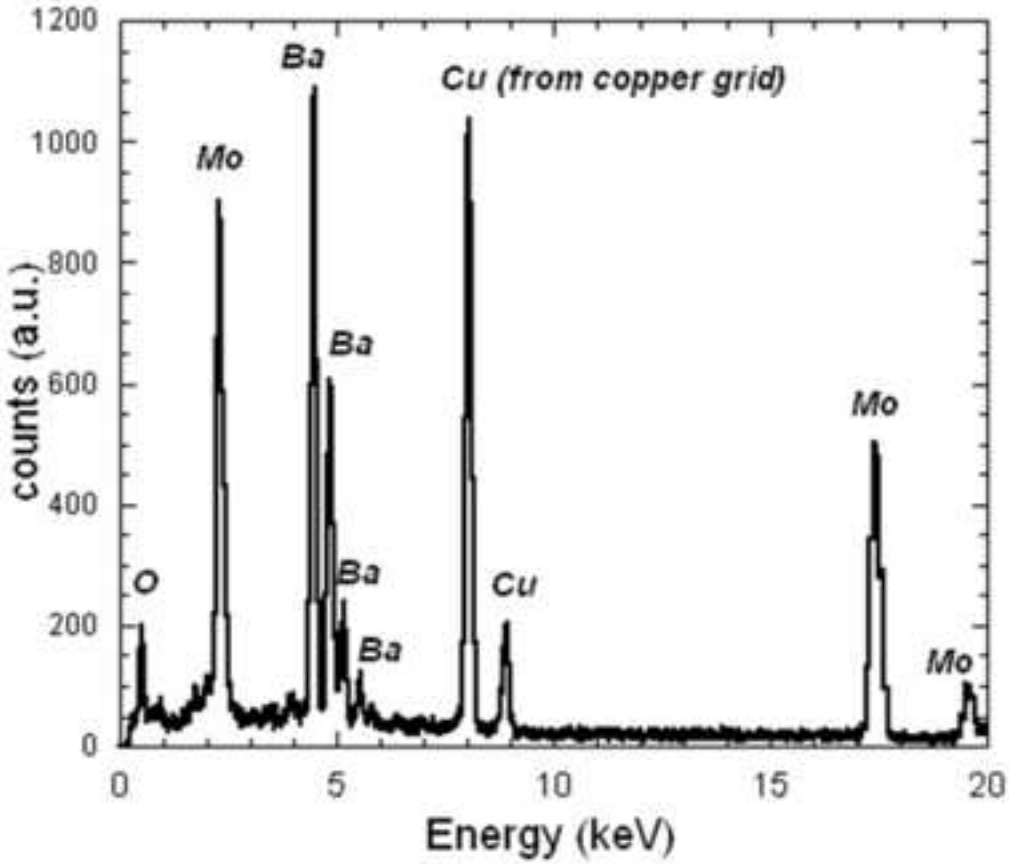

b)

Figure5
Click here to download high resolution image

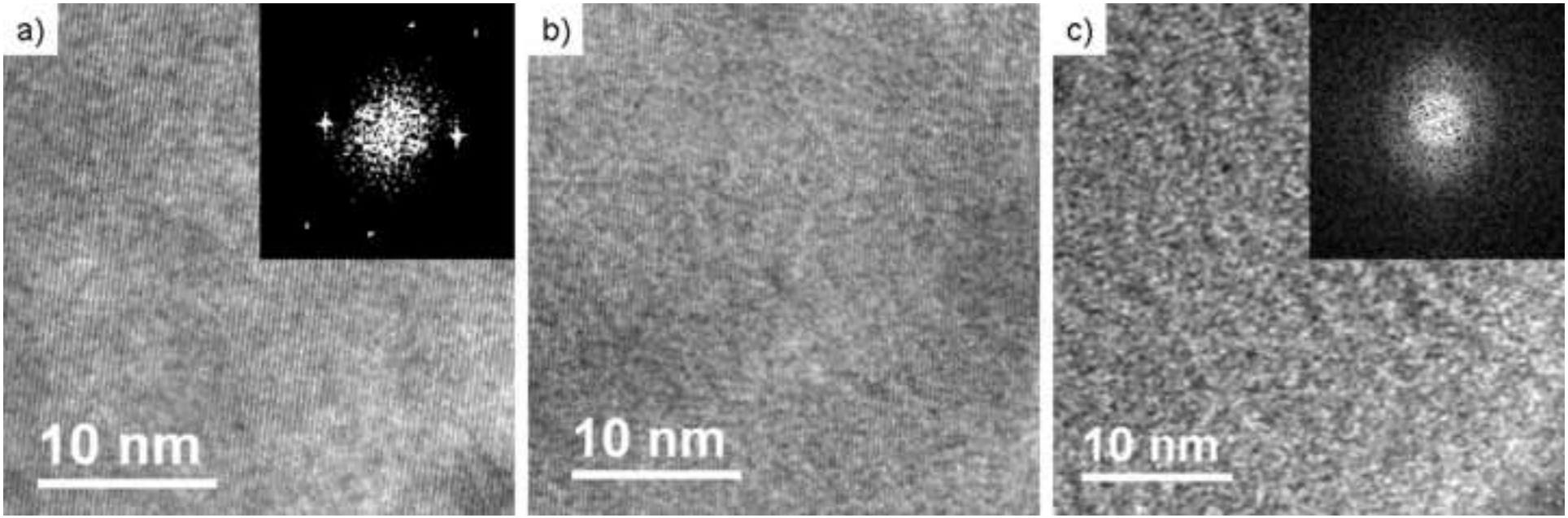

Figure6

Click here to download high resolution image

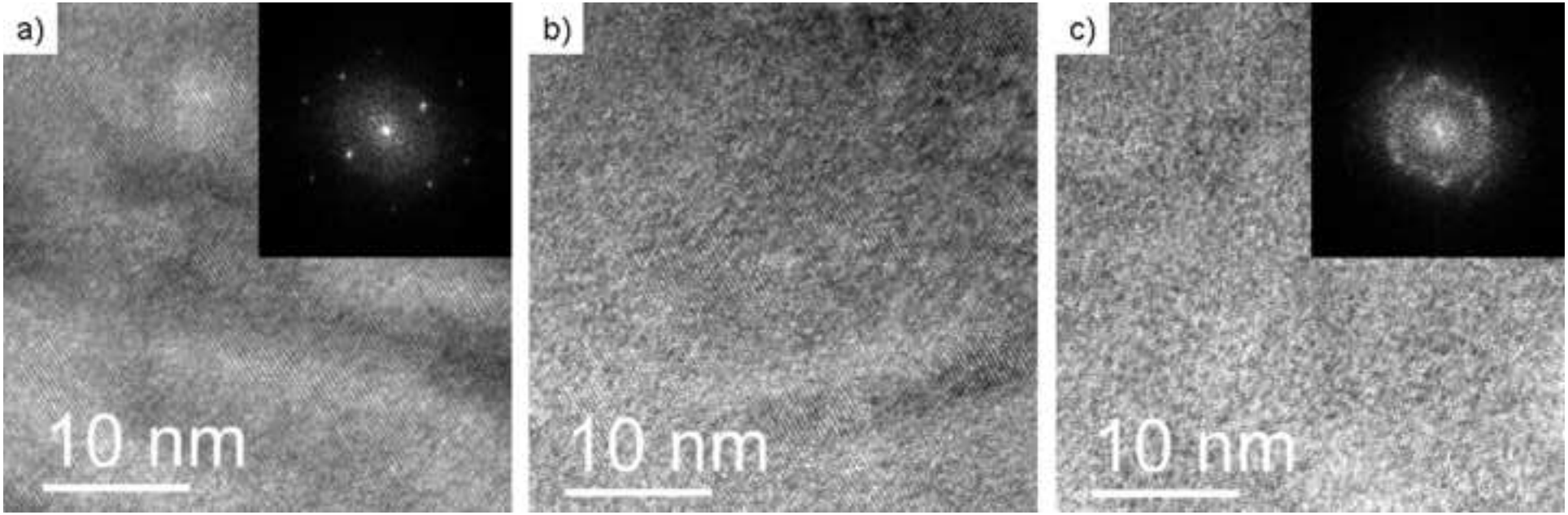

Figure7

Click here to download high resolution image

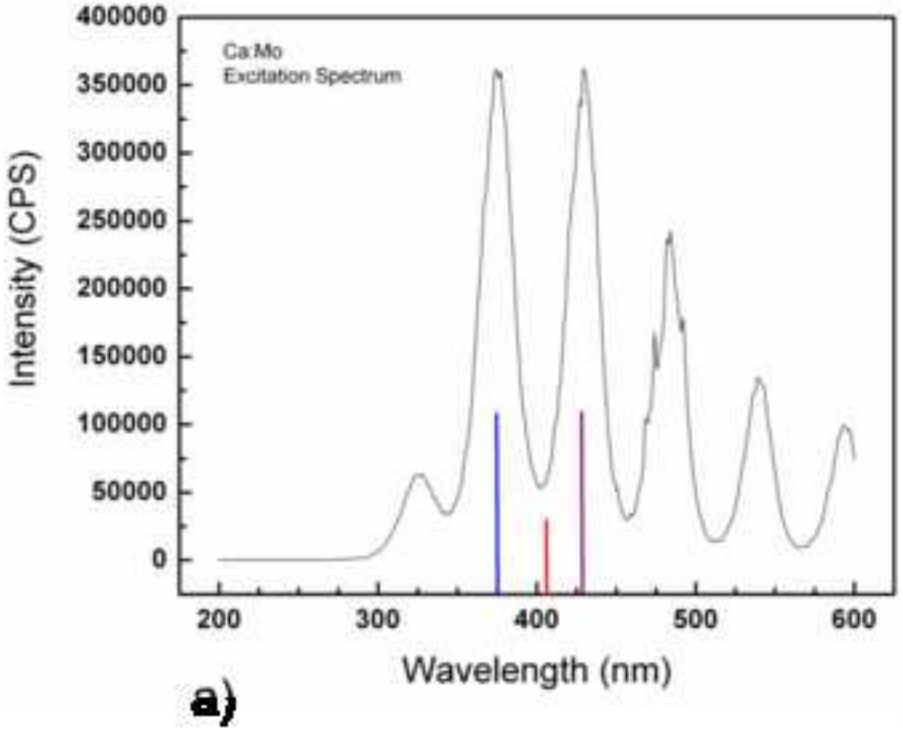

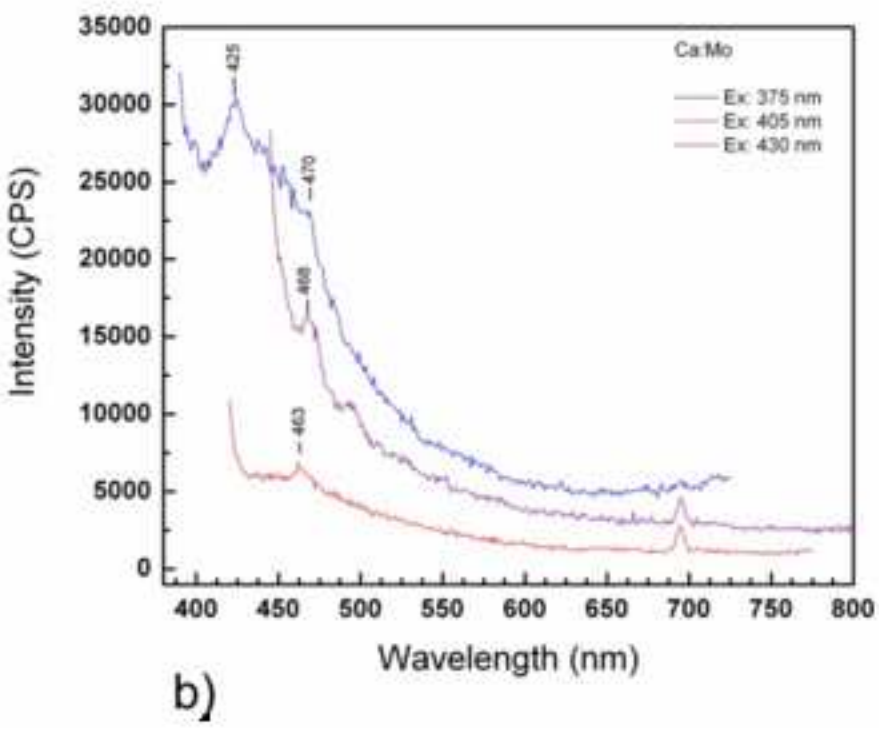

Figure8

Click here to download high resolution image

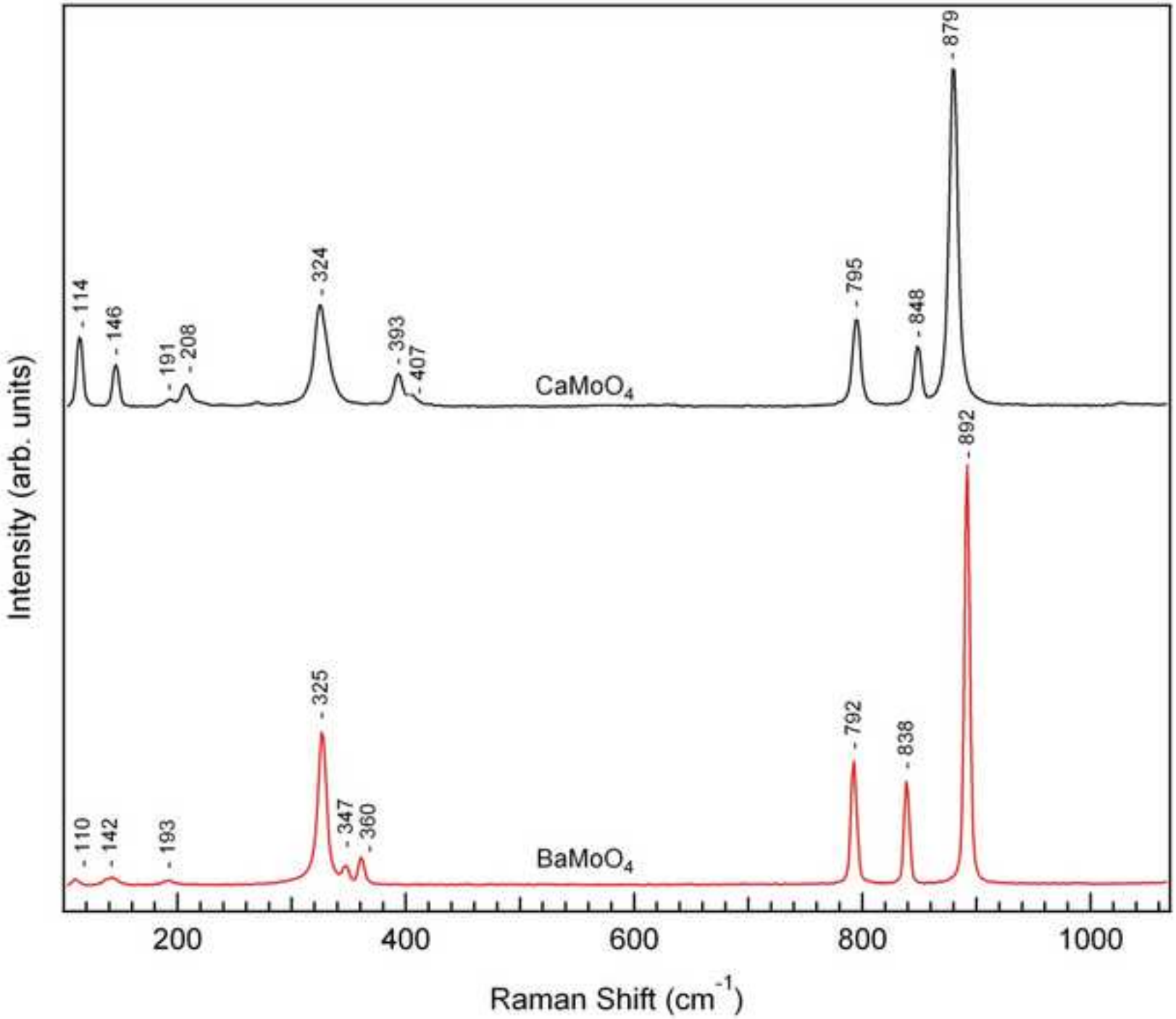

Figure9

Click here to download high resolution image